Talanta 188 (2018) 507–515

Contents lists available at ScienceDirect

Talanta

journal homepage: www.elsevier.com/locate/talanta

Simultaneous and highly sensitive detection of multiple breast cancer biomarkers in real samples using a SERS microfluidic chip

Zhihua Zheng, Lei Wu, Lang Li, Shenfei Zong, Zhuyuan Wang*, Yiping Cui

Advanced Photonics Center, Southeast University, Nanjing 210096, China

ARTICLE INFO

Keywords:
SERS
Microfluidic chip
Immunoassay
Biomarkers
Real sample

ABSTRACT

Accurate and quantitative analysis of breast cancer biomarkers is a particularly requisite in the early diagnosis of breast cancers, especially in real samples. Here, we develop a surface enhanced Raman scattering (SERS) immunoassay biosensor based on a microfluidic chip for the simultaneous detection of multiple breast cancer biomarkers in real samples. In such an immunoassay, immuno-Ag aggregates are labeled with different Raman reporters to detect multiple breast cancer biomarkers in real samples. Moreover, to better enhance the Raman signals, self-assembled silver nanoparticles are introduced on the bottom of the microfluidic channels to obtain the SERS active immune-substrate. In order to avoid the crosstalk of SERS signals, we designed a spatially separated detection biosensor by using multi-channels in a microfluidic chip. In the experiments, CA153, CA125 and CEA are selected as the models of breast cancer biomarkers, which can be simultaneously detected of in human serum with an excellently specificity and a high sensitivity. Furthermore, the proposed SERS microfluidic biosensor can be applied to detect the biomarkers in real samples using a linear regression method for the statistical analysis. Our detection results are in agreement with those obtained using commercial ELISA kits, which proves the reliability of our SERS-based microfluidic immunoassay.

1. Introduction

Although there is a growing understanding of breast cancer progression and the therapeutic modalities are more and more diverse, breast cancer mortality is still very high [1,2]. One reason is that patients are diagnosed with breast cancers quite late [3]. Therefore, it is critical to improve the accuracy of early diagnosis of breast cancers, which can sufficiently improve the overall survival rates [4].

So far, enormous research results have confirmed that tumor biomarkers have a great potential in early diagnosis and monitoring of cancers [5]. Due to the diversity of breast cancers, diagnosis depending on only one kind of tumor biomarker is usually inaccurate [6]. Previous results have indicated that the simultaneous detection of breast cancer biomarkers, including carbohydrate antigen 15-3 (CA153), carbohydrate antigen 12-5 (CA125) and carcinoembryonic antigen (CEA) can greatly improve the accuracy of diagnosis. As a result, developing an immunoassay biosensor that can simultaneously detect multiple tumor biomarkers is of cardinal significance [7,8].

Generally, the concentrations of biomarkers in the peripheral blood of early-stage breast cancer patients are relatively low (CA153 < 30 U/mL, CA125 < 35 U/mL, CEA < 10 ng/mL). At present, common methods to detect cancer biomarkers include enzyme-linked immunosorbent assay (ELISA), electrochemical (EC), electrochemiluminescence (ECL), surface plasmon resonance (SPR), *etc.* [9–13]. For example, Grzywa et al. used avian lgY antibodies to detect CA153 with ELISA technique, achieving a sensitivity of 0.028 U/mL in PBS [14]. Andrea et al. developed a micro-flow label-free impedimetric biosensor based on thin-film interdigitated gold array microelectrodes for the detection of CA125. The developed immunosensor showed a good analytical performance and the limit of detection (LOD) reached 7 U/mL in PBS [15]. Pang et al. constructed a highly sensitive ECL sensor to detect CEA, and the LOD was 0.02 ng/mL in PBS [16]. These biosensors provided potential tools for cancer diagnosis. However, it would be more meaningful to develop novel techniques which enable the detection of biomarkers in real physiological environment. Raamanathan et al. reported a programmable Bio-Nano-Chip system for quantitative detection of CA125 in serum with a fluorescence-based sandwich immunoassay, and the LOD was 1 U/mL in human serum [17]. Despite the rapid and significant progress in this research field, it is still extremely challenging to design a facile biosensor with a high sensitivity and accuracy for testing multiple biomarkers in real samples.

Since 1990s, the SERS has become one of the most attractive analytical tools for immunoassay [18–24]. It was found that when the analytes adsorbed on the rough metal surfaces, especially on the

* Corresponding author.
E-mail address: wangzy@seu.edu.cn (Z. Wang).

https://doi.org/10.1016/j.talanta.2018.06.013
Received 30 December 2017; Received in revised form 22 April 2018; Accepted 4 June 2018
Available online 06 June 2018
0039-9140/

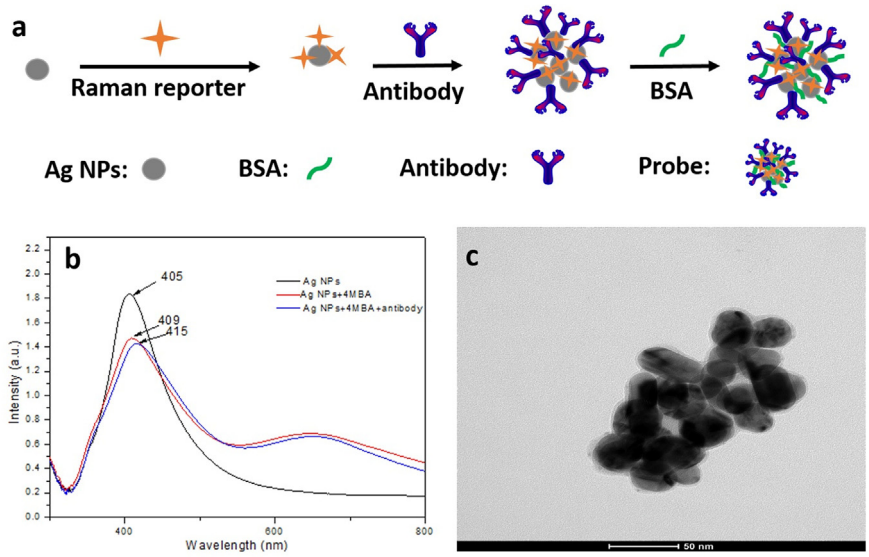

Fig. 1. Preparation and characterization of the SERS probes. (a) Fabrication procedures of the SERS probes. (b) Extinction spectra of Ag NPs, 4MBA-labeled Ag NPs and SERS probes. c. TEM image of the SERS probes.

aggregates of metal NPs, the intensity of Raman signals can be greatly enhanced [25–27]. In addition, SERS technique is advantageous in the applications of multiplex detection due to its fingerprint characteristics [28]. Thus, among the various detection techniques of immunoassays, SERS has gained an increasing attract in recent decades. Typically, a SERS immunoassay is developed by a "Sandwich" structure, which is similar to that in an ELISA immunoassay [29,30]. In that scheme, usually a flat glass surface is first immobilized with the capture antibodies. Meanwhile, metal nanoparticles are labeled with Raman reporters and conjugated with detection antibodies to generate SERS probes. Then, the target antigens can be captured by the antibodies on the substrate and subsequently be detected by the signals from SERS probes [31]. Interestingly, it has been reported that by introducing a SERS-activated substrate in the immunoassay structure, the detecting sensitivity can be further increased [32]. Previously, we have developed a SERS-based sandwich immunoassay by utilizing a SERS-active immune substrate. The detection sensitivity was increased by about 3 orders compared with that of a immunoassay without a SERS-active substrate [33].

However, due to the relatively low reproducibility and nonspecific adsorption, there is still a great requirement to develop SERS-based multiplex immunoassay with a high sensitivity for the detection in real samples [34]. Fortunately, in the last decade, microfluidic immunoassays, which improve the reproducibility and specificity, have been widely used in biology, chemistry and medicine. The microfluidic chips also provides advantages including small size, high throughput, fast reaction rates, ease of integration and low sample consumption [35–39]. Consequently, combining SERS with microfluidic chip for immunoassays has opened the door for new opportunities where both technique can profit [40–42]. Recently, using a SERS-assisted 3D barcode chip, we have presented a microfluidic biosensor for multiplex sensing [43]. By combining the SERS spectral encoding technique with the microfluidic spatial encoding, a simultaneous detection of multiple targets in multiple samples was achieved.

Here, we design an improved microfluidic biosensor for the multiple detection of breast cancer biomarkers, which can be used in real samples with a high sensitivity. In such an immunoassay scheme, Ag nanoparticles (Ag NPs) were immobilized onto the microfluidic channels to form a SERS-active substrate, which can further increase the detection sensitivity due to the enhanced SERS activity. Then the specific antibodies were attached on the different regions of the SERS substrate to capture the target biomarkers. To recognize the species and concentration of the biomarkers, Raman reporter-labeled immuno-Ag aggregates were used as the SERS probes [44,45]. With target biomarker presented in the sample, a sandwich type immune-complex will form between the SERS substrate, biomarker and SERS probe. By comparing the SERS intensities in different regions of the SERS substrate, both qualitatively and quantitatively analysis of the breast cancer biomarkers can be realized. In the experiment, CA153, CA125 and CEA, three kinds of important breast cancer biomarkers, were detected simultaneously, which has a great medical significance for the early detection of breast cancers. Finally and importantly, real blood from the patients were also employed to evaluate the detection accuracy and practicability of the demonstrated biosensor.

2. Experimental

2.1. Materials and chemicals

The PDMS chip was fabricated by Suzhou Wenhao Chip Tech. Co., Ltd. The ELISA kits, CA153, CA125, CEA and anti-CA153, anti-CA125 and anti-CEA antibodies were purchased from Shanghai Linc-Bio Science Co. LTD. 4MBA, DTNB and 2NAT were purchased from Sigma-Aldrich. Tween 20 and ethanol were purchased from Sinopharm Chemical Reagent Co., Ltd. Polyethyleneimine (PEI, M.W. 10000) and glutaraldehyde (GA, 50% aqueous solution) were purchased from Alfa Aesar. Borate buffered saline (BBS) was purchased from Nanjing Chemical Reagent Co., Ltd. Sulfuric acid (H_2SO_4, 98%) was purchased from Shanghai Lingfeng Chemical Co., Ltd. Hydrogen peroxide (H_2O_2, 30%) was purchased Aladdin Industrial Inc. Phosphate buffered saline (PBS, 0.01 M, pH 7.4) were purchased from Beijing Biosynthesis Biotechnology Co., Ltd. Bovine serum albumin (BSA) was purchased from Invitrogen Biotechnology Co., Ltd. The buffer solutions were as follows: BBS, 2 mM, pH = 9. Phosphate buffered saline tween-20 (PBST), 0.05% tween 20 in 10 mM PBS, pH = 7.4.

2.2. Preparation of DTNB-labeled Ag NPs

First, 390 mL of deionized water with 72 mg $AgNO_3$ was heated to boil at 130 °C under stirring. Second, 10 mL of 1% sodium citrate solution was added and the mixture was heated until the solution became yellow-green. Then the solution was cooled down to room temperature for future use. Third, 6 mL of the as-prepared Ag NPs solution was centrifuged at 11,000 rpm for 30 min and the precipitates was

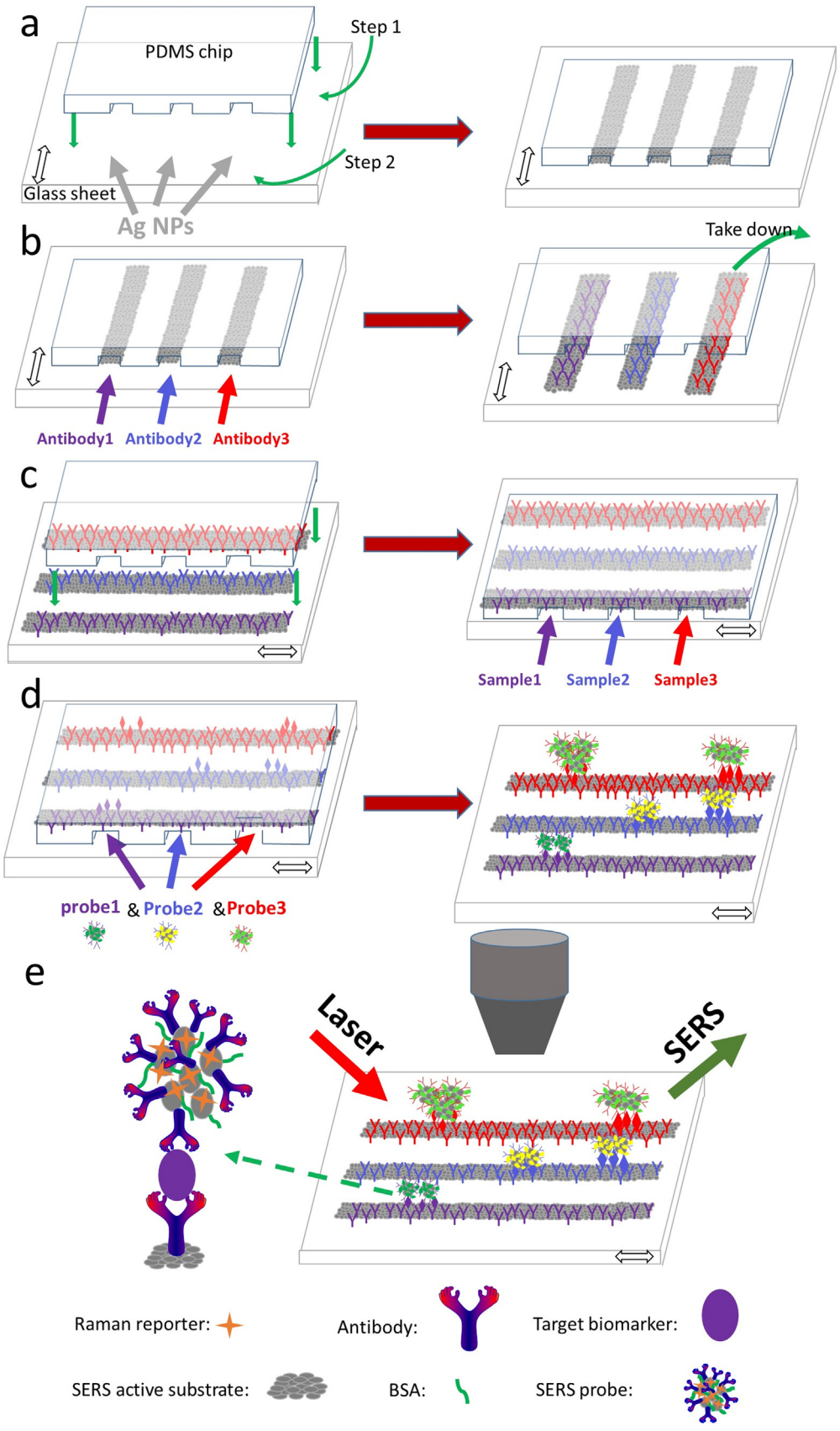

Fig. 2. Schematic diagram of the experimental procedures. (a) Illustration of the microfluidic system. Polydimethylsiloxane (PDMS) chip was bonded to the glass sheet. Ag NPs were injected into the microfluidic channels by syringe pumps. (b) Different capture antibodies were injected into the Ag NPs modified microfluidic channels *via* syringe pumps. (c) The previous PDMS chip was removed and a new PDMS chip was bonded to the glass sheet perpendicular to the previous placement. Different samples were injected into the microfluidic channels. (d) The mixture of three kinds of SERS probes was injected into the microfluidic channels. (e) The sandwich structure formed in the microfluidic channels and SERS signal of each crossing region (*i.e.* the reaction spot) was measured with a confocal microscope.

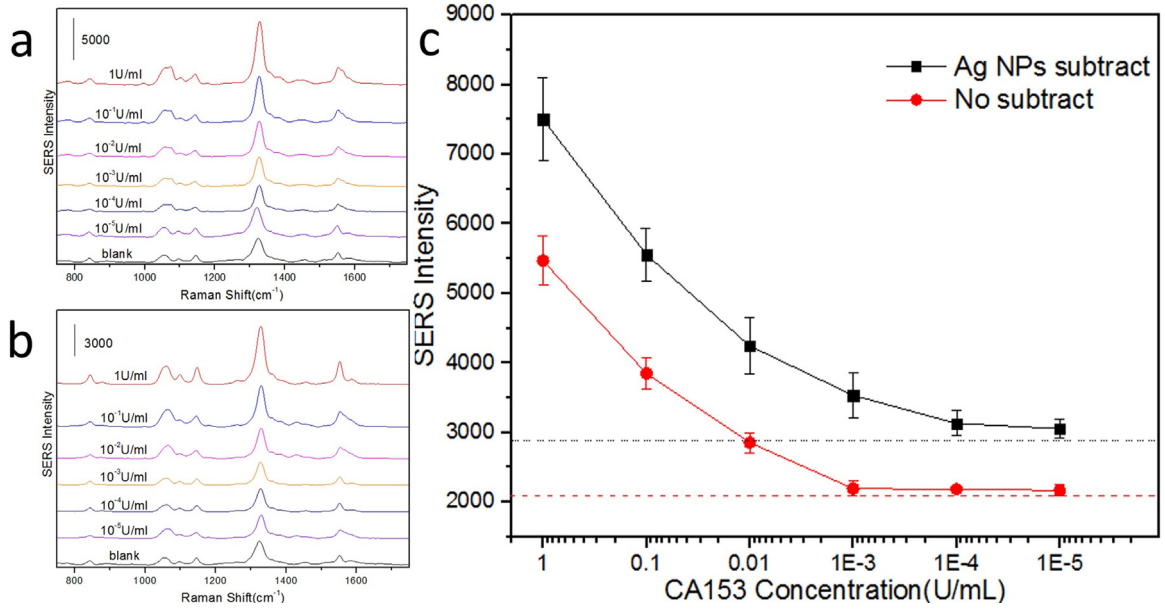

Fig. 3. Detection sensitivity of the microfluidic biosensor. (a) Concentration-dependent SERS spectra for CA153 suspended in phosphate buffered saline (PBS) using the SERS active substrate in the microfluidic channel. (b) Concentration-dependent SERS spectra for CA153 suspended in PBS with no SERS active substrate in the microfluidic channel. (c) Plot of the peak intensity at 1333 cm^{-1} as a function of CA153 concentrations. The black and red lines represent microfluidic biosensors with or without SERS active substrate, respectively.

redispersed in 4 mL of deionized water. Afterwards, 40 μL of 10 mM DTNB solution was added to the solution of Ag NPs and stirred for 2 h, followed by a centrifugation at 9000 rpm for 20 min. The precipitates were re-dispersed in 1.0 mL of BBS solution. The fabrication process of 4MBA- and 2NAT-labeled Ag NPs is similar to that of DTNB-labeled Ag NPs (see Sections 1 and 3 in the Supporting information).

2.3. Fabrication of immuno-SERS probes

Here, we take the process of preparing mouse anti-CA153-conjugated SERS probes as an example. The method for fabricating anti-CA125- or anti-CEA-modified SERS probes is similar to that of anti-CA153-conjugated SERS probes (see Sections 2 and 4 in the Supporting information). First, 50 μL of 0.05 mg/mL mouse anti-CA153 antibody (in BBS) was added to 1 mL of the as-prepared DTNB-labeled Ag NPs. And the mixture was placed at 4 ℃ for 2 h. Second, after centrifuged at 6500 rpm for 12 min, the precipitates of the DTNB-labeled immune-Ag NPs were re-dispersed in 1 mL of BBS solution. After that, 10 μL of 5% BSA solution was added to the mixture and reacted for 1 h at 4 ℃. Finally, the mixture was centrifuged at 6500 rpm for 12 min and the precipitates were suspended in 200 μL of BBS solution and stored at 4 ℃ for future use.

2.4. Preparation of SERS-active substrate in microfluidic channels

The glass sheet was soaked in 98% H_2SO_4 and 30% H_2O_2 (volume ratio 3:1) mixture beforehand. When used, the glass sheet was flushed with a large volume of deionized water and then dried with N_2 and put into the oven at 80 ℃. The PDMS chip was immersed in absolute ethanol and sonicated for 2 h. Then the PDMS chip was washed with plenty of deionized water and dried with N_2. The above steps were repeated at least twice. Next, the PDMS chip was placed in an oven at 80 ℃ for 2 h. Finally, the PDMS chip and the glass sheet were bonded together. The bonding between PDMS and glass using the hot bonding method, which can increase the force between molecules and increase the effect of thermal diffusion, thus creating a reliable bonding between PDMS and glass. More detail of bonding and removing process were shown in Fig. S2 in Supplementary information.

To prepare the substrates deposited with Ag NPs in microfluidic channels, 1% PDDA solution was injected into the microfluidic channel using a syringe pump working at a rate of 0.5 μL/min for 30 min. Then the solution of Ag NPs was injected into the microfluidic channel with the same rate for 30 min. Since PDDA was decomposed in water, the chloride ions were broken down, and remaining polymer was positively charged, which can be used to absorb the negatively charged Ag NPs. Using this layer-by-layer method, we could form the SERS-active substrate. Then, the above steps were repeated once to increase the density of Ag NPs for a better SERS performance. After that, 1% PEI and 2% GA solution were subsequently injected into the microfluidic channels for 1 h at a rate of 0.5 μL/min.

Afterwards, 0.01 mg/mL of antibody (mouse anti-CA153/CA125/CEA, in PBS) was injected into the microfluidic channel at a rate of 0.5 μL/min for 40 min. Then the chip was allowed to stand for 30 min to ensure that the antibody can fully attach to the surfaces of Ag NPs. Next, 5% BSA (in PBS) was injected at a rate of 2 μL/min for 3 min to wash away the excess antibodies. Then the injection rate was changed to 0.5 μL/min for 25 min. BSA is used to prevent the non-specific adsorption. After carefully removing the PDMA chip from the glass sheet, the liquid on the substrate was allow to dry naturally at room temperature. Eventually, a new piece of PDMS chip was bonded with the glass sheet. Especially, the channel of the PDMS chip was perpendicular to the SERS active channels.

2.5. Immunoassay protocol

A SERS-based immunoassay in microfluidic channels was performed as follows. BSA, samples and immuno-SERS probes were sequentially injected into the microfluidic channel at a rate of 0.5 μL/m for 40 min. All of the samples in this experiment were spiked in 5% serum solution. After each injection, the chip was allowed to stand for 30 min. PBST was injected into the microfluidic channel at a rate of 2 μL/m for 5 min at the end of standing. After completing all of the above steps, the reagents in the microfluidic channel were discharged with air and then subjected to SERS measurements. The PDMS chip did not need to be removed from the glass sheet and it was detected directly using a confocal microscope after processing.

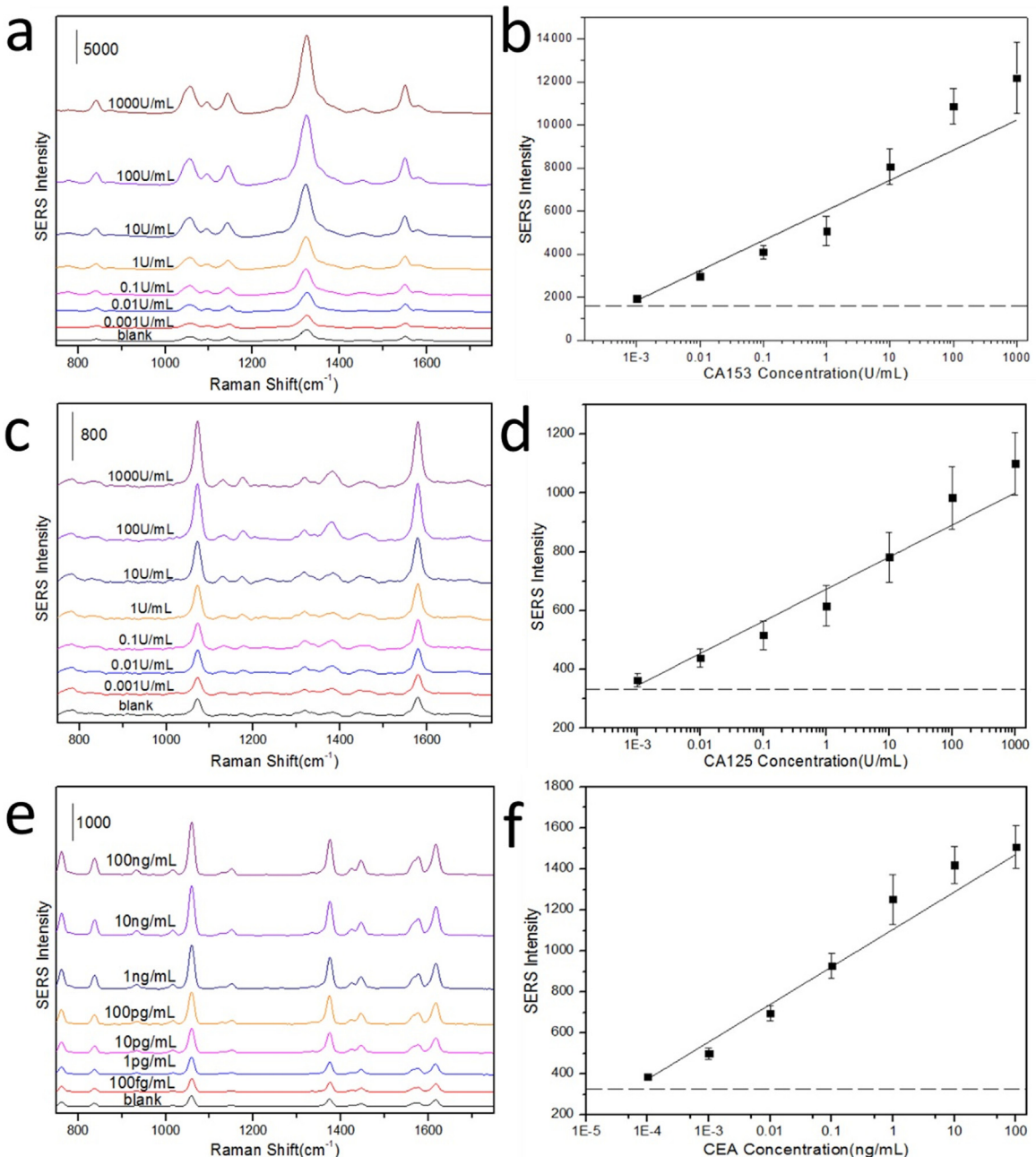

Fig. 4. Quantitative analysis of three types of breast cancer biomarkers, respectively. (a) Concentration-dependent SERS spectra for CA153 (0.001 U/mL to 1 kU/mL, in serum). (b) Calibration curve for CA153. Plot of peak intensity at 1333 cm^{-1} as a function of CA153 concentration. (c) Concentration-dependent SERS spectra for CA125 (0.001 U/mL to 1 kU/mL, in serum). (d) Calibration curve for CA125. Plot of peak intensity at 1080 cm^{-1} as a function of CA125 concentration. (e) Concentration-dependent SERS spectra for CEA (100 pg/mL to 100 ng/mL, in serum). (f) Calibration curve for CEA. Plot of peak intensity at 1378 cm^{-1} as a function of CEA concentration.

2.6. Instruments

Samples were centrifuged using a centrifuge (3–30 K, Sigma, Germany). The syringe pumps (LongerPump, LSP04-1A and LSP02-1B) were used to inject reagents to the microfluidic channels. SERS signals were measured by a confocal microscope (FV 1000, Olympus) with a 10× objective lens (NA = 0.4) and a spectrograph (Sharmrock, Andor, UK) with Newton 303i charge-coupled device (CCD). The SERS spectra were obtained with an integration time of 60 s. UV–vis spectrophotometer (UV-3600, Shimadzu, Japan) was used to measure the extinction spectra. Field emission scanning electron microscopy (SEM) (Sirion200, PEI, Holand) with 20 kV accelerating voltage was used to characterize the morphology of the SERS probes. Transmission electron microscopy (TEM) images characterizing the morphology of the SERS probe were obtained by a transmission electron microscopy (JEM 2000 EX, Jeol, USA) operating at 120 kV accelerating voltage.

3. Results and discussion

3.1. Preparation and characterization of the SERS probes

For preparing the immune-SERS probes, Ag NPs were modified with Raman reporters (4-mercaptobenzoic acid, 4MBA) and specific antibodies (Fig. 1(a)). The TEM image and the size distribution result of Ag NPs are shown in Fig. S1, which indicates that the average size of Ag NPs is about 53 nm. Both 4MBA and antibodies attached to the surfaces

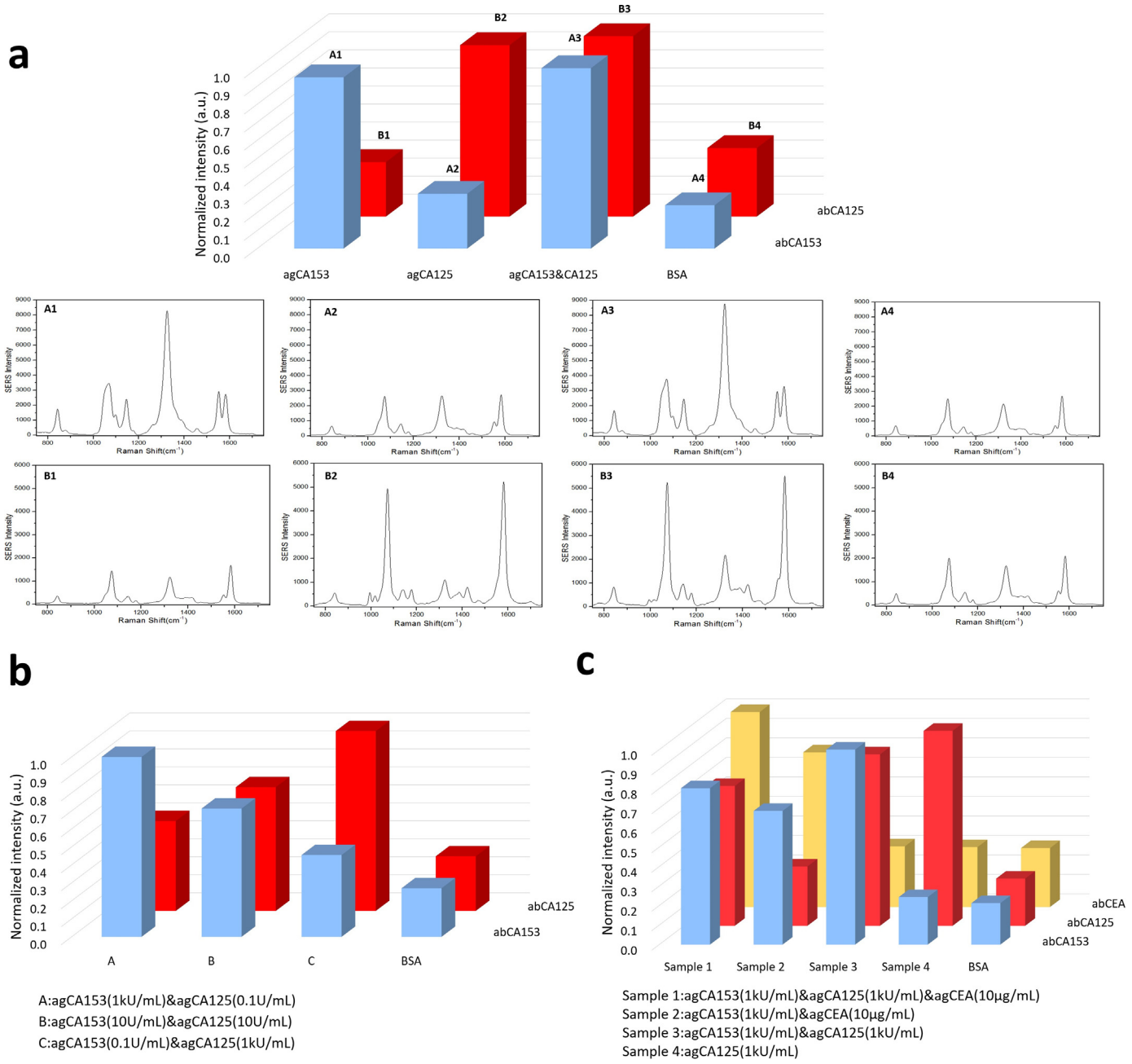

Fig. 5. (a) Detection results of CA153 and CA125. 5% BSA was used as the control. The heights of the bar graph represent the intensity of the immuno-SERS probes (anti-CA153-conjugated SERS probes at 1333 cm^{-1} and anti-CA125-conjugated probes at 1080 cm^{-1}). The SERS intensities have been normalized by the maximum peak intensity of each channel modified with the same kind of antibodies. (b) Quantitative detection results of CA153 and CA125 in four samples. Sample 1 contains CA153 (1 kU/mL, in serum) and CA125 (1 U/mL, in serum), Sample 2 contains CA153 (10 U/mL, in serum) and CA125 (10 U/mL, in serum), Sample 3 contains CA153 (0.1 U/mL, in serum) and CA125 (1 kU/mL, in serum), Sample 4 contains only BSA (5%) (the blank control). The heights of the bar graph represent the intensity of the SERS probes (CA153 probe at 1333 cm^{-1} and CA125 probes at 1080 cm^{-1}). The SERS intensities have been normalized by the maximum peak intensity of each channel modified with the same kind of antibodies. (c) Simultaneous detection of CA153, CA125 and CEA. 5% BSA was used as a blank control. The heights of the bar graph represent the intensity of the SERS probes (CA153 probe at 1333 cm^{-1}, CA125 probes at 1080 cm^{-1} and CEA probes at 1378 cm^{-1}). The SERS intensities have been normalized by the maximum peak intensity of each channel modified with the same kind of antibodies.

of Ag NPs through Ag–S bonds. The interaction between Ag NPs and 4MBA molecules to form the Ag–S bond is a chemical interaction. In order to prove the formation of Ag–S bond, we have measured the Raman signal of Ag NPs and 4MBA-labeled Ag NPs, respectively. The comparative results show that after 4MBA were attached to the surfaces of Ag NPs, a Raman peak at 236 cm^{-1} appeared, indicating of the formation of Ag–S bond. This result is in agreement with that previously reported [46,47].

In our experiments, to detect CA153, CA125 and CEA simultaneously, 4MBA, DTNB and 2NAT molecules were used to generate SERS probes with different SERS spectra, which were conjugated with anti-CA153, anti-CA125 and anti-CEA antibodies, respectively. Besides, bovine serum albumin (BSA) was used to block the non-specific adhesion sites on the immune-SERS probes. As shown in Fig. 1(b), the extinction peak of Ag NPs located at 405 nm. After being modified with 4MBA molecules, the extinction peak red-shifted to 409 nm. Besides, an obvious bump occurred at around 670 nm, which suggests the formation of Ag NPs aggregates [48]. Further, after being conjugated with

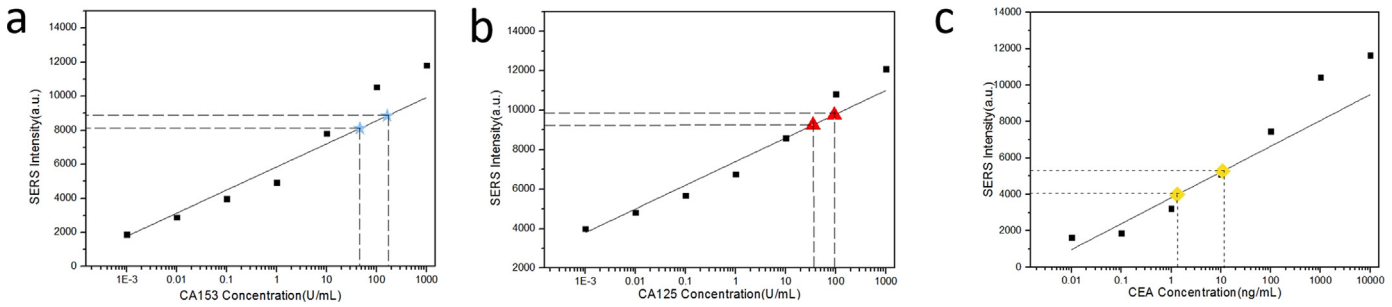

Fig. 6. The biosensor was used to detect three kinds of biomarkers in real samples. (a) Standard curve for detecting CA153 (0.001 U/mL to 1 kU/mL, in serum) and real samples obtained using SERS intensities at 1333 cm^{-1}. (b) Standard curve for detecting CA125 (0.001 U/mL to 1 kU/mL, in serum) and real samples obtained using SERS intensities at 1080 cm^{-1}. (c) Standard curve for detecting CEA (0.1 pg/mL to 100 ng/mL, in serum) and real samples obtained using SERS intensities at 1378 cm^{-1}.

Table 1
The equation of CA153, CA125 and CEA standard curve and linear degree.

Biomarker	Intercept	Slope	R
CA153	5852.01474	1356.06420	0.96298
CA125	7406.40830	1200.21825	0.97455
CEA	3812.14718	1417.23714	0.95582

antibodies, the extinction peak red-shifted to 415 nm. TEM images were also used to investigate the morphology of immune-SERS probes. As shown in Fig. 1(c), the prepared SERS probes was formed by multiple Ag NPs.

3.2. SERS-based microfluidic biosensor

Fig. 2 briefly illustrates the experimental procedures. As shown in Fig. 2(a), this microfluidic biosensor mainly consists of a PDMS chip and a glass sheet. The injection of reagents was controlled by syringe pumps. As described in the experimental session, Ag NPs were first immobilized onto the glass sheet through the electrostatic adsorption, forming a SERS-active substrate. SEM image of the SERS active substrate in the channel was shown in Fig. S3, which indicates that Ag NPs are successfully deposited on the bottom of the channels by forming a layer of ~150 nm height. Then the capture antibodies, samples and immune-SERS probes were sequentially injected into the channels (Fig. 2(b)–(d)). If the sample contains the target biomarker specific to the antibodies on the substrate, a typical type of sandwich immune-structure would be formed due to the antigen-antibody binding (Fig. 2(e)). Then, the concentration of each biomarker can be determined by the intensity of the corresponding SERS signals.

3.3. Detection strategy

By using multiple antibodies and channels, this kind of SERS-based microfluidic chip is capable of detecting high throughput samples. Specifically, if there are y kinds of biomarkers in *x* samples to be tested, an Ag NPs substrate needs to be prepared with *y* parallel microfluidic channels and *y* kinds of the corresponding antibodies need to be injected into each channel, respectively. Afterwards, another PDMS chip is to be bonded to the glass sheet in the direction vertical to that of the channels deposited with Ag NPs. Then *x* types of samples were separately injected into each channel, followed by the injection of y kinds of SERS probes, respectively. The SERS signal in each reaction region is measured to determine the concentration of each target biomarker in each sample.

3.4. Biosensing capability of the fabricated SERS active substrate

Further, to increase the detecting sensitivity, a SERS active substrate were introduced in the microfluidic channels using self-assembled Ag NPs. Such a SERS substrate can effectively enhance Raman signals, which makes it possible to achieve a lower detection limit. A preliminary experiment has been conducted to investigate the influence of the added SERS substrate by using CA153 as a model sample. In the experiments, a microfluidic chip with a bottom of pure glass was used as a control. Specifically, the solution of anti-CA153 antibody, CA153 ($1–10^{-5}$ U/mL, in PBS), CA153 specific SERS probes (Raman reporter: 5,5′-dithiobis (2-nitrobenzoic acid), DTNB) were sequentially injected into the microfluidic channels. Especially, when using the control microfluidic chip, the injection time, rate and other conditions were kept all the same for comparison. Finally, SERS signal of each crossing region (reaction region) was measured and the results are shown in Fig. 3. As can be seen, when the SERS active substrate was used the limit of detection (LOD) of CA153 (in PBS) could reach as low as 0.0001 U/mL, two orders of magnitude lower than that of the microfluidic chip without SERS substrate. Thus, the detection sensitivity of the microfluidic chip can be remarkably increased due to the addition of a SERS active substrate on the bottom of the channels.

3.5. Quantitative analysis of three types of breast cancer biomarkers

Next, the sensitivity of the biosensor was investigated for detecting three different kinds of breast cancer biomarkers in serum individually. As demonstrated in Experimental Section, three kinds of immuno-SERS probes were fabricated using DTNB, 4MBA and 2-naphthalenthiol (2NAT) as Raman reporters, which were conjugated with anti-CA153, anti-CA125 and anti-CEA antibodies, respectively, for detecting CA153, CA125 and CEA. The SERS spectra of three kinds of immune-SERS probes are shown in Fig. S4. For investigating the quantitative detecting ability of the chip, the serum solutions with a concentration of CA153

Table 2
The actual values and the measured results of biomarkers.

Sample	GENDER/AGE	CA153 (U/mL)		CA125 (U/mL)		CEA (ng/mL)	
		Actual value	Measured value	Actual value	Measures value	Actual value	Measures value
1	Female/40	142.5	193.1	85.5	92.7	8.1	12.0
2	Female/37	32.5	47.9	14.4	26.1	1.2	1.7

ranging from 0.01 U/mL to 1 kU/mL were injected into the microfluidic channels. The SERS results are shown in Fig. 4(a), which shows that the intensity of SERS signals increased concomitantly with the increasing concentrations of CA153. The concentration-dependent SERS spectra were further studied by plotting of the SERS intensity at 1333 cm^{-1} as a function of the logarithm of CA153 concentration (Fig. 4(b)). Similarly, the detection sensitivities of CA125 (Fig. 4(c), (d)) and CEA (Fig. 4(e), (f)) were also determined using the microfluidic biosensor. As can be seen from Fig. 4(b), (d), (f), the concentration of the tumor biomarkers exhibit a good linear relationship with the SERS intensity. The calibration equations of CA153, CA125 and CEA are as follows,

$$\text{CA153: } Y = 1398.00433 \times \log X + 6033.00489$$

$$\text{CA125: } Y = 109.11075 \times \log X + 673.30984$$

$$\text{CEA: } Y = 141.72372 \times \log X + 381.21471$$

According to Fig. 4, the LODs of CA153 and CA125 are both 0.01 U/mL while that of CEA reached about 1 pg/mL. Compared with previously reported results, these values of LODs for the detection of CA153, CA125 and CEA in serum were much lower (see Tables S1–S3, Supporting information), which benefit from the intense SERS signal of the immune-SERS probes, the additional Raman enhancement provided by the SERS active substrate. Since the content of CA153, CA125 and CEA in normal human serum is at the level of ~ 30 U/mL, ~ 35 U/mL and ~ 10 ng/mL, respective [21,49], such a low LODs of this microfluidic biosensor should be sufficient for the practical clinical applications.

3.6. Simultaneous and highly sensitive detection of multiple breast cancer biomarkers

Afterwards, in order to verify the feasibility of this method to detect two kinds of tumor biomarkers simultaneously, CA153 and CA125 were analyzed using the proposed microfluidic biosensor. Fig. 5(a) shows the results for the qualitative detection of CA153 and CA125 in four samples. In the experiments, first, anti-CA153 antibodies and anti-CA125 antibodies were conjugated to two parallel channels deposited with Ag NPs, respectively. Then Sample 1 to Sample 4 with different contents were perpendicularly injected into the channels. Here, Sample 1 contained both CA153 and CA125 (1 kU/mL, in serum); Sample 2 contained CA153 (1 kU/mL, in serum); Sample 3 contained CA125 (1 kU/mL, in serum); Sample 4 contained BSA (5%) and was used as a blank control. Finally, the SERS immuno-probes were injected into the channels to form sandwich structures. As shown in Fig. 5(a), with target biomarkers present in the sample, the intensity of SERS signal in the corresponding region should be much stronger than that in the region without the target. For example, the SERS intensity in region A1 and A2 was much higher than that in A3 and A4, because CA153 was only contained in Sample 1 and 2. For region A3 and A4, although there was no CA153 existed, weak SERS signals was still observed due to the non-specific adsorption of SERS immuno-probes on the bottom of the channels. The above results showed that the rational designed microfluidic biosensor could be used for the simultaneous detection of CA153 and CA125 in 4 different samples.

After that, the performance of the microfluidic biosensor in the simultaneous and quantitative detection of two different biomarkers was evaluated. As shown in Fig. 5(b), two parallel SERS immuno-substrate channels were first prepared by immobilizing anti-CA153 and anti-CA125 antibodies onto two parallel Ag NPs substrates respectively. Then four samples containing CA125 and CA153 mixed at different concentrations ratios were perpendicularly injected into the SERS immuno-substrate channels. Other steps were the same as previously described. As can be seen from Fig. 5(b), the heights of the histogram, indicating the intensity of SERS signals, were well in accordance with the concentrations of the two biomarkers. And the two biomarkers mixed at different concentrations could be quantified using this microfluidic biosensor according to the SERS intensities. These experimental results indicated that the biosensor can be used to perform the simultaneous quantitative analysis of two biomarkers, which is of great importance in the clinical diagnosis applications. In order to verify the effectiveness of the microfluidic biosensor, a standard recovery experiment were also supplied (see Fig. S5, Supporting information). The experimental results show that our proposed microfluidic biosensor has relative good reproducibility.

Afterwards, the ability of this microfluidic biosensor to simultaneously detect three different biomarkers in different samples in serum was investigated. A similar method was used as shown in Fig. 2. Specifically, three specific capture antibodies (anti-CA153, anti-CA125 and anti-CEA antibodies were modified on three parallel SERS active channels, respectively. Then 5 samples in serum containing various combinations of CA125, CA153 and CEA were separately injected into 5 channels, as illustrated in Fig. 5(c). Sample 1 contained CA153 (1 kU/mL), CA125 (1 kU/mL) and CEA (10 μg/mL); Sample 2 contained CA153 (1 kU/mL) and CEA (10 μg/mL); Sample 3 contained CA153 (1 kU/mL) and CA125 (1 kU/mL); Sample 4 contained only CA125 (1 kU/mL); Sample 5 contained only BSA (5%). Then, a mixture of anti-CA153 SERS probe, anti-CA125 SERS probe and anti-CEA SERS probes was simultaneously injected into each of the five microfluidic channels. If the target sample contains biomarkers specific to the capture antibodies on the SERS substrate, there should show the corresponding SERS signals with a higher intensity. Thus, by comparing the SERS intensity of each reaction region, whether the sample contains the corresponding biomarkers can be determined. As shown in Fig. 5(c), for the SERS active channel conjugated with anti-CA153 antibodies, the SERS intensity of Sample 1, Sample 2 and Sample 3 was significantly stronger than that of Sample 4 and Sample 5. Thereby, it can be conclude that Sample 1, Sample 2 and Sample 3 contained CA153, in good agreement with the sample contents. So this biosensor can simultaneously detect three different kinds of biomarkers in serum. And in order to investigate the reproducibility and long-term stability of the proposed microfluidic biosensor, a long-term stabilized experiment was also performed using 4MBA as reporters (see Fig. S6, Supporting information). In the experiments, 21 of such microfluidic biosensors were prepared. Then, one biosensor were used for the detection of 4MBA molecules after each two days. Within the observed 21 days, although the SERS intensity decreased with time, the SERS activity of the microfluidic chip remained strong enough to be used as a biosensor.

3.7. Real sample detection

Finally, to evaluate the detection accuracy and practicability of this microfluidic biosensor in clinical applications, these three kinds of biomarkers in real samples from two people were detected. In the first step, a calibrating curve of the immunoassay was obtained using the standard CA153 samples (0.001 U/mL to 1 kU/mL, in serum). Then the SERS intensities of each reaction area were collected. As shown in Fig. 6(a), a standard calibration curve for CA153 and real samples was obtained using the SERS intensities at 1333 cm^{-1}. A similar method was used to detect CA125 and CEA in human serum (Figs. 6(b) and 6(c)). The calibration equations of CA153, CA125 and CEA are as follows.

$$\text{CA153: } Y = 1356.06420 \times \log X + 5852.01474 \quad (1)$$

$$\text{CA125: } Y = 1200.21825 \times \log X + 7406.40830 \quad (2)$$

$$\text{CEA: } Y = 1417.23714 \times \log X + 3812.14718 \quad (3)$$

where Y is the SERS intensity of the band at 1333, 1080 and 1378 cm^{-1}, respectively. X is the concentration of CA153, CA125 and CEA, respectively. The R (correlation coefficient) of CA153, CA125 and CEA standard curve were 0.96298, 0.97455 and 0.95582. This means

the concentration of the three kinds of biomarkers in real samples has a good linear relationship with the SERS intensities. The measured concentration of the three kinds of biomarkers in sample 1 and sample 2 were obtained by comparing the SERS intensities of sample 1 and sample 2 at 1333, 1080 and 1378 cm^{-1} using the Eqs. (1)–(3), respectively. As shown in Table 1 and 2, the measured values were close to the actual values for the three kinds of biomarkers. This result confirms the detection accuracy and practicability of the microfluidic biosensor.

4. Conclusions

In this study, we proposed a SERS-based microfluidic biosensor for the simultaneous detection of multiple breast cancer biomarkers in real samples. With the SERS active substrates patterned in the microfluidic channels, the sensitivity could be improved by two orders of magnitude. Due to the excellent SERS enhancement effect, the LOD of CA153 could reach 0.0001 U/mL in buffer solution. The biosensor also enables the simultaneous detection of multiple breast cancer biomarkers in human serum. The LOD of CA153, CA125 and CEA reached 0.01 U/mL, 0.01 U/mL and 1 pg/mL in serum, respectively, which are lower than the cutoff values for clinical diagnosis. The practicability of this biosensor was tested by the quantitative detection of CA153, CA125 and CEA in real samples. The results obtained from the proposed SERS-microfluidic chip are close to those obtained using commercial ELISA kits, which demonstrated the accuracy of this biosensor for the practical use. All the above-mentioned merits of the biosensor suggest that such a microfluidic biosensor would have an attractive application in clinical diagnosis.

Acknowledgement

This research was supported by the State Key Program of National Natural Science of China (Grant no. 61535003), the National Key Basic Research Program of China (Grant no. 2015CB352002), the Excellent Youth Foundation of Jiangsu Province (BK20140023), the National Natural Science Foundation of China (NSFC) (Nos. 61675042, 61505027), the Fundamental Research Funds for the Central Universities.

Appendix A. Supplementary material

Supplementary data associated with this article can be found in the online version at http://dx.doi.org/10.1016/j.talanta.2018.06.013.

References

[1] S.F. Kingsmore, I.E. Lindquist, J. Mudge, D.D. Gessler, W.D. Beavis, Nat. Rev. Drug Discov. 7 (2008) 221–230.
[2] F. Bray, J.-S. Ren, E. Masuyer, J. Ferlay, Int. J. Cancer 132 (2013) 1133–1145.
[3] K.R. Bauer, M. Brown, R.D. Cress, C.A. Parise, V. Caggiano, Cancer 109 (2007) 1721–1728.
[4] C. Hughes, G. Clemens, B. Bird, T. Dawson, K.M. Ashton, M.D. Jenkinson, A. Brodbelt, M. Weida, E. Fotheringham, M. Barre, J. Rowlette, M.J. Baker, Sci. Rep. 6 (2016).
[5] J.F. Rusling, C.V. Kumar, J.S. Gutkind, V. Patel, Analyst 135 (2010) 2496–2511.
[6] K.K. Reza, J. Wang, R. Vaidyanathan, S. Dey, Y. Wang, M. Trau, Small 13 (2017).
[7] Y.-H. Wen, P.-Y. Chang, C.-M. Hsu, H.-Y. Wang, C.-T. Chiu, J.-J. Lu, Clin. Chim. Acta 450 (2015) 273–276.
[8] J. Wu, Z. Fu, F. Yan, H. Ju, Trac-Trends Anal. Chem. 26 (2007) 679–688.
[9] J. Homola, Chem. Rev. 108 (2008) 462–493.
[10] J. Homola, Anal. Bioanal. Chem. 377 (2003) 528–539.
[11] I. Nishizono, S. Iida, N. Suzuki, H. Kawada, H. Murakami, Y. Ashihara, M. Okada, Clin. Chem. 37 (1991) 1639–1644.
[12] M. Lee, S. Lee, J.-H. Lee, H.-W. Lim, G.H. Seong, E.K. Lee, S.-I. Chang, C.H. Oh, J. Choo, Biosens. Bioelectron. 26 (2011) 2135–2141.
[13] J. Li, Z. Skeete, S. Shan, S. Yan, K. Kurzatkowska, W. Zhao, Q.M. Ngo, P. Holubovska, J. Luo, M. Hepel, C.-J. Zhong, Anal. Chem. 87 (2015) 10698–10702.
[14] R. Grzywa, A. Lupicka-Slowik, M. Walczak, M. Idzi, K. Bobrek, S. Boivin, A. Gawel, T. Stefaniak, J. Oleksyszyn, M. Sienczyk, Altex-Altern. Anim. Exp. 31 (2014) 43–52.
[15] A. Ravalli, L. Lozzi, G. Marrazza, Curr. Drug Deliv. 13 (2016) 400–408.
[16] X. Pang, J. Li, Y. Zhao, D. Wu, Y. Zhang, B. Du, H. Ma, Q. Wei, Acs Appl. Mater. Interfaces 7 (2015) 19260–19267.
[17] A. Raamanathan, G.W. Simmons, N. Christodoulides, P.N. Floriano, W.B. Furmaga, S.W. Redding, K.H. Lu, R.C. Bast Jr., J.T. McDevitt, Cancer Prev. Res. 5 (2012) 706–716.
[18] X.Y. Zhang, M.A. Young, O. Lyandres, R.P. Van Duyne, J. Am. Chem. Soc. 127 (2005) 4484–4489.
[19] F. Yan, T. Vo-Dinh, Sens. Actuators B-Chem. 121 (2007) 61–66.
[20] L. Yang, M.X. Gao, L. Zhan, M. Gong, S.J. Zhen, C.Z. Huang, Nanoscale 9 (2017) 2640–2645.
[21] M. Li, J.W. Kang, S. Sukumar, R.R. Dasari, I. Barman, Chem. Sci. 6 (2015) 3906–3914.
[22] Y. Ma, K. Pronithaveepong, N. Li, Acs Appl. Mater. Interfaces 9 (2017) 10530–10536.
[23] X. Wu, Y. Xia, Y. Huang, J. Li, H. Ruan, T. Chen, L. Luo, Z. Shen, A. Wu, Acs Appl. Mater. Interfaces 8 (2016) 19928–19938.
[24] X. Fu, Z. Cheng, J. Yu, P. Choo, L. Chen, J. Choo, Biosens. Bioelectron. 78 (2016) 530–537.
[25] D.L. Jeanmaire, R.P. Vanduyne, J. Electroanal. Chem. 84 (1977) 1–20.
[26] Z. Li, K. Zhu, Q. Zhao, A. Meng, Appl. Surf. Sci. 377 (2016) 23–29.
[27] Z. Zhang, J. Yu, J. Yang, X. Lv, T. Wang, Appl. Surf. Sci. 359 (2015) 853–859.
[28] Z. Cheng, N. Choi, R. Wang, S. Lee, K.C. Moon, S.-Y. Yoon, L. Chen, J. Choo, Acs Nano 11 (2017) 4926–4933.
[29] D.D. Usta, K. Salimi, A. Pinar, I. Coban, T. Tekinay, A. Tuncel, Acs Appl. Mater. Interfaces 8 (2016) 11934–11944.
[30] W. Wang, W. Wang, L. Liu, L. Xu, H. Kuang, J. Zhu, C. Xu, Acs Appl. Mater. Interfaces 8 (2016) 15591–15597.
[31] J. Ni, R.J. Lipert, G.B. Dawson, M.D. Porter, Anal. Chem. 71 (1999) 4903–4908.
[32] Y. Pei, Z. Wang, S. Zong, Y. Cui, J. Mater. Chem. B 1 (2013) 3992–3998.
[33] C. Song, Z. Wang, R. Zhang, J. Yang, X. Tan, Y. Cui, Biosens. Bioelectron. 25 (2009) 826–831.
[34] A.H. Nguyen, J. Lee, H.I. Choi, H.S. Kwak, S.J. Sim, Biosens. Bioelectron. 70 (2015) 358–365.
[35] T.M. Squires, S.R. Quake, Rev. Mod. Phys. 77 (2005) 977–1026.
[36] S.-Y. Teh, R. Lin, L.-H. Hung, A.P. Lee, Lab Chip 8 (2008) 198–220.
[37] J. Narang, N. Malhotra, C. Singhal, A. Mathur, D. Chakraborty, A. Anil, A. Ingle, C.S. Pundir, Biosens. Bioelectron. 88 (2017) 249–257.
[38] A. Hasan, J. Saliba, H.P. Modarres, A. Bakhaty, A. Nasajpour, M.R.K. Mofrad, A. Sanati-Nezhad, Biomaterials 103 (2016) 278–292.
[39] J. Sun, Y. Xianyu, X. Jiang, Chem. Soc. Rev. 43 (2014) 6239–6253.
[40] I.J. Jahn, O. Zukovskaja, X.S. Zheng, K. Weber, T.W. Bocklitz, D. Cialla-May, J. Popp, Analyst 142 (2017) 1022–1047.
[41] R. Gao, J. Ko, K. Cha, J.H. Jeon, G.-e. Rhie, J. Choi, A.J. deMello, J. Choo, Biosens. Bioelectron. 72 (2015) 230–236.
[42] R. Gao, Z. Cheng, A.J. deMello, J. Choo, Lab Chip 16 (2016) 1022–1029.
[43] L. Wu, Z. Wang, K. Fan, S. Zong, Y. Cui, Small 11 (2015) 2798–2806.
[44] Y. Wang, B. Yan, L. Chen, Chem. Rev. 113 (2013) 1391–1428.
[45] X. Fu, L. Chen, J. Choo, Anal. Chem. 89 (2017) 124–137.
[46] I. Matulaitiene, Z. Kuodis, A. Matijoska, O. Eicher-Lorka, G. Niaura, J. Phys. Chem. C 119 (2015) 26481–26492.
[47] I. Matulaitiene, L. Abariute, Z. Kuodis, O. Eicher-Lorka, A. Matijoska, G. Niaura, Chemija 25 (2014) 13–19.
[48] O.D. Bekasova, A.A. Brekhovskikh, A.A. Revina, V.T. Dubinchuk, Inorg. Mater. 44 (2008) 835–841.
[49] H. Kobayashi, Y. Yamada, T. Sado, M. Sakata, S. Yoshida, R. Kawaguchi, S. Kanayama, H. Shigetomi, S. Haruta, Y. Tsuji, S. Ueda, T. Kitanaka, H. Oi, Gynecol. Obstet. Investig. 65 (2008) 133–138.